Timosaponin A-III Induces Autophagy Preceding Mitochondria-Mediated Apoptosis in HeLa Cancer Cells

Lai-King Sy,[1,2] Siu-Cheong Yan,[1,2] Chun-Nam Lok,[1] Ricky Y.K. Man,[2] and Chi-Ming Che[1]

[1]Department of Chemistry and Open Laboratory of Chemical Biology of the Institute of Molecular Technology for Drug Discovery and Synthesis, and [2]Department of Pharmacology, The University of Hong Kong, Hong Kong, China

Abstract

Timosaponin A-III (TAIII), a saponin isolated from the rhizome of *Anemarrhena asphodeloides*, exhibits potent cytotoxicity and has the potential to be developed as an anticancer agent. Here, we provide evidence that TAIII induces autophagy in HeLa cells followed by apoptotic cell death. TAIII-induced autophagy was morphologically characterized by the formation of membrane-bound autophagic vacuoles recognizable at the ultrastructural level. TAIII-treated cells expressing green fluorescent protein (GFP)–labeled microtubule-associated protein 1 light chain 3 (LC3) displayed punctate fluorescence indicative of LC3 recruitment to the autophagosome. This was associated with the conversion of LC3-I (the cytosolic form) into LC3-II (the lipidated form located on the autophagosome membrane). TAIII treatment also induced mitochondrial dysfunction involving overproduction of reactive oxygen species and reduction of mitochondrial membrane potential accompanied by induction of mitochondrial permeability transition. Prolonged exposure to TAIII resulted in cytochrome *c* release and caspase-3 activation, events that signified the onset of apoptotic cell death. TAIII-induced autophagy preceded apoptosis, as evidenced by early autophagic vacuole formation, GFP-LC3 translocation, and LC3-II increase in the absence of caspase-3 cleavage. Notably, TAIII-mediated apoptotic cell death was potentiated by treatment with autophagy inhibitor 3-methyladenine or small interfering RNA against the autophagic gene *beclin 1*. These findings suggest that TAIII-elicited autophagic response plays a protective role that impedes the eventual cell death. In terms of structure-activity relationship, the sugar chain in TAIII is indispensable to the drug action, as the sugar-lacking aglycone sarsasapogenin did not induce autophagy and exhibited weaker cytotoxicity. [Cancer Res 2008;68(24):10229–37]

Introduction

Evidence is accumulating to prove that saponins can inhibit tumor cell proliferation, with great potential to be developed as chemotherapeutic agents (1, 2). *Anemarrhena asphodeloides* Bge. (Liliaceae), containing saponins as the major and biological active components, is a traditional Chinese medicine reported to be efficacious in treating diabetes and inhibiting platelet aggregation (3). A notable saponin isolated from *A. asphodeloides* is timosaponin A-III (TAIII), a spirostanol saponin consisting of a disaccharide moiety attached to the C_3 position of the aglycone sarsasapogenin (Fig. 1*A*). Sarsasapogenin does not have the double bond at C_5 and C_6 and structurally resembles the aglycones of dioscin and polyphyllin D, which were previously reported to exhibit anticancer activities (1, 2). TAIII was shown to suppress arachidonic acid–induced superoxide generation in human neutrophils (4) and increase the intracellular Ca^{2+} concentration in endothelial cells (5). Nevertheless, the anticancer potential of TAIII has not been explored.

The mode of cytotoxic action of anticancer drugs often involves the induction of programmed cell death (PCD). Apoptosis (type I PCD) is characterized by chromatin condensation, nuclear breakdown, DNA fragmentation, and activation of caspases. Autophagy (type II PCD) is a highly conserved process in eukaryotic cells from yeast to mammals (6). In autophagy, bulk cytoplasm including cellular organelles such as mitochondria, fractured endoplasmic reticulum, and peroxisomes is sequestered by a phagophore, which encloses and develops into a double- or multi-membrane autophagosome. On fusion with lysosome, the autophagosome further develops into an autolysosome, where the cellular constituents are degraded by lysosomal hydrolases (7). Autophagy is recognized as a cellular process by which the cytoplasmic materials such as damaged organelles or long-lived proteins are degraded and recycled into energy and nutrients when cells are stressed by hypoxia (8), radiation (9, 10), chemical insults (11–14), or nutritional deprivation (15). The importance of autophagy is also reflected by its involvement in human pathologies such as muscular disorders (16), aging (17), and neurodegenerative diseases (18). A number of anticancer drugs such as arsenic trioxide (11), tamoxifen (19), and mTOR inhibitor rapamycin (20) are, in fact, effective autophagy-inducing agents.

Here we show for the first time that TAIII induced autophagy in HeLa cells, followed by mitochondria-dependent apoptotic cell death. TAIII-induced mitochondrial dysfunction, as shown by increased production of reactive oxygen species (ROS), reduction of mitochondrial membrane potential ($\Delta\psi_m$), induction of mitochondrial permeability transition (MPT), release of cytochrome *c*, and activation of caspase-3, seems to be instrumental in triggering autophagy/apoptosis. The inhibition of autophagy by treatment with 3-methyladenine (3-MA) or *beclin 1* small interfering RNA (siRNA) sensitized the cells to apoptosis, revealing that TAIII-induced autophagy is protective in nature and precedes the apoptotic cell death. Our findings suggest that TAIII is a potent cytotoxic saponin that can be added to the emerging list of autophagy-inducing agents with potential to be developed as cancer chemotherapeutic agents.

Note: Supplementary data for this article are available at Cancer Research Online (http://cancerres.aacrjournals.org/).

L-K. Sy and S-C. Yan contributed equally to this work.

Requests for reprints: Chi-Ming Che, Department of Chemistry and Open Laboratory of Chemical Biology, Institute of Molecular Technology for Drug Discovery and Synthesis, The University of Hong Kong, Pokfulam Road, Hong Kong, SAR, China. Phone: 852-28592154; Fax: 852-28571586; E-mail: cmche@hku.hk.

doi:10.1158/0008-5472.CAN-08-1983

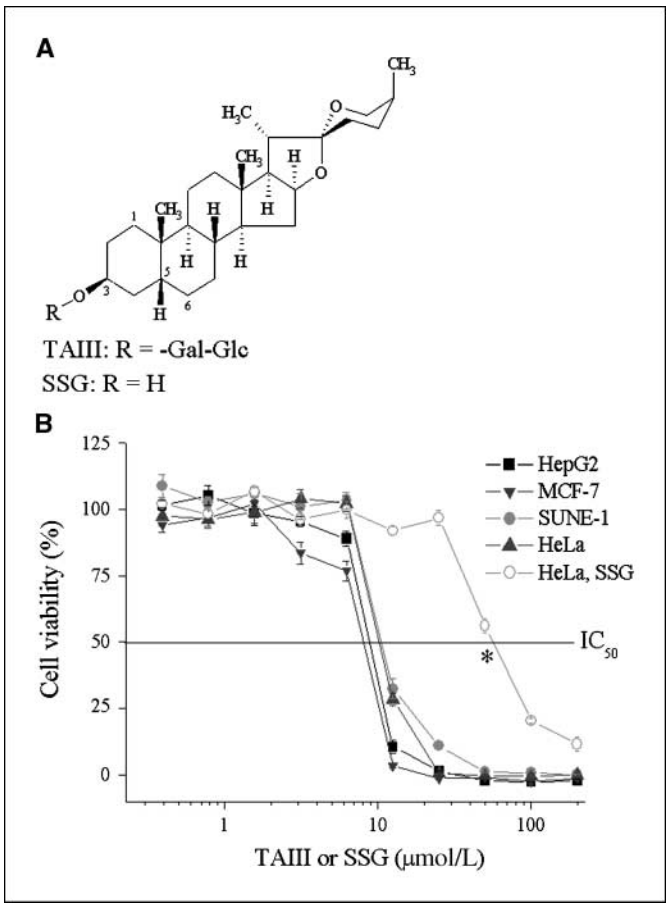

Figure 1. TAIII exhibits cytotoxic effects against various cancer cell lines whereas the aglycone sarsasapogenin (*SSG*) exhibits relatively weaker cytotoxic effect to HeLa cancer cells. *A,* TAIII consists of hydrophobic (spirostanol aglycone, sarsasapogenin) and hydrophilic (disaccharide) moieties. *B,* the cytotoxic effects of TAIII in HepG2, MCF-7, SUNE-1, and HeLa cancer cell lines and the cytotoxic effect of sarsasapogenin in HeLa cells after 48-h incubation were determined using MTT assay. *, $P < 0.05$, compared with the IC_{50} of TAIII treatment in HeLa cells.

Materials and Methods

Reagents. All reagents were of analytic grade (purity > 98%) and were purchased from Sigma-Aldrich Chemical Co. unless otherwise specified. TAIII and cyclosporin A were purchased from Wako Pure Chemical Industries, Ltd. TAIII was purified before biological use. TAIII and sarsasapogenin dissolved in DMSO were used as stock solutions. Cell culture medium constituents were purchased from Life Technologies, Inc. Cell Proliferation Kit I (MTT) was purchased from Roche. The antibody against microtubule-associated protein 1 light chain 3 (LC3) was from Abgent; antibodies against Beclin 1, caspase-9, caspase-3, and cytochrome *c* were from Cell Signaling Technology; the antibody against actin was from Abcam.

Cell lines and cell culture. HeLa, HepG2, and MCF-7 cell lines were obtained from American Type Culture Collection and maintained in minimum essential medium supplemented with fetal bovine serum (10%), nonessential amino acids (0.1 mmol/L), L-glutamine (2 mmol/L), penicillin (100 units/mL), and streptomycin (100 μg/mL). SUNE-1 was provided by Prof. S.W. Tsao (Department of Anatomy, The University of Hong Kong, Hong Kong, SAR, China) and maintained in supplemented RPMI 1640. Cultures were incubated in a humidified atmosphere of 95% air and 5% CO_2 at 37°C.

Cell viability assay. Cells (8×10^3 per well) were seeded in supplemented culture medium (100 μL/well) in 96-well plates and incubated for 24 h. Then the medium was replaced with a drug-containing medium, and the cells were further incubated for 24 to 48 h. All experiments were run in parallel with controls (0.2% DMSO) and the cell viabilities were evaluated by MTT assays. The absorbance of formazan formed was measured at 580 nm by a microplate analyzer (Perkin-Elmer Fusion α-FP).

Transmission electron microscopy. HeLa cells treated with DMSO, TAIII, or sarsasapogenin were collected by trypsinization, washed twice with PBS, and then fixed with 0.5 mL of ice-cold glutaraldehyde (2.5% in 0.1 mol/L cacodylate buffer, pH 7.4) at 4°C overnight. After washing, cells were postfixed in OsO_4 (0.5 mL, 1%) and embedded in Polybed resin. Ultrathin sections were doubly stained with uranyl acetate and lead citrate and analyzed by transmission electron microscopy (208S Philips).

Examination of LC3 translocation. HeLa cells (1×10^5) were plated in 35-mm glass-bottomed dishes with supplemented culture medium and incubated for 24 h. Cells were transfected with green fluorescent protein (GFP)–labeled LC3 (1 μg) using the GeneJuice transfection reagent (Novagen) and incubated for another 24 h for the expression of GFP-LC3 fusion protein. The localization of LC3 in transfected cells was examined by fluorescence microscopy (Zeiss Axiovert 200M).

Immunoblotting. TAIII-treated HeLa cells were lysed with a solution containing Tris-HCl (100 mmol/L, pH 6.8), SDS (4% w/v), glycerol (20%), and dithiothreitol (20 mmol/L), supplemented with protease inhibitor and nuclease mix. The lysate was centrifuged at 10,000 × *g* for 30 min. Equal amounts of the protein (50 μg) were resolved by SDS-PAGE (12.5%) and transferred onto a polyvinylidene fluoride membrane (Immobilion-P). The membrane was blocked with a buffer containing Tris (10 mmol/L, pH 7.4), NaCl (150 mmol/L), Tween 20 (0.1%), and bovine serum albumin (5%) and then incubated with the primary antibodies at 4°C overnight. The membrane was washed and treated with appropriate secondary antibody for 2 h. The immunoreactivities were detected with the enhanced chemiluminescence plus kit (GE Healthcare). Cytosolic fractions for cytochrome *c* detection were obtained with a reagent kit (Pierce). Actins were probed to ensure equal protein loading.

Determination of ROS levels. Intracellular ROS were determined by measuring the intracellular oxidation of nonfluorescent dihydrorhodamine-123 (DHRh-123) to green fluorescent rhodamine-123 (Rh-123). Cells (8×10^3 per well) were cultured in 96-well black-bottomed plates for 24 h. TAIII was added for the indicated time points. Cells were washed once with HBSS and incubated with DHRh-123 (5 μmol/L) in HBSS for 30 min. After washing, the cell-associated fluorescence was measured with a microplate analyzer with excitation and emission wavelengths of 488 and 530 nm, respectively.

Determination of superoxide dismutase and catalase activities. Experiments were done according to the manufacturer's protocols (Cayman). Briefly, HeLa cells (1×10^6) were seeded in 100-mm dishes with supplemented culture medium and incubated overnight. Cells treated with DMSO or TAIII were harvested at the specified time, washed with PBS, and pelleted by centrifugation at 500 × *g* for 5 min. The cell pellet was sonicated in 1 mL of ice-cold buffer [50 mmol/L potassium phosphate (pH 7.0) containing 1 mmol/L EDTA] and centrifuged at 10,000 × *g* at 4°C for 15 min. The supernatant was collected for protein determination and superoxide dismutase (SOD) and catalase analyses.

Measurement of mitochondrial membrane potential ($\Delta\psi_m$). The mitochondrial membrane potential probe, Rh-123, is taken up by mitochondria and fluoresces in a $\Delta\psi_m$-dependent manner. Cells (8×10^3 per well) were cultured in 96-well black-bottomed plate for 24 h. TAIII was added for the indicated time intervals. Cells were washed once with HBSS and then incubated with Rh-123 (1 μmol/L) in HBSS for 30 min. After washing, Rh-123 fluorescence was measured using a microplate analyzer with excitation and emission wavelengths at 488 and 530 nm, respectively.

Localization of mitochondrial ROS and detection of MPT. HeLa cells (4×10^5) were cultured in glass-bottomed dishes with supplemented culture medium and incubated for 24 h. Cells were treated with DMSO or TAIII (10 μmol/L) for 6 h and stained with MitoTracker Red (50 nmol/L, Molecular Probes) for 2 min at 37°C and washed. For ROS localization, cells were stained with 2′,7′-dichlorofluorescin diacetate (DCFDA; 15 μmol/L) for 2 min at 37°C. For MPT detection, cells were incubated with calcein-AM (1 μmol/L, Molecular Probes) and $CoCl_2$ (5 mmol/L) for 15 min at 37°C. After washing with PBS, cell images were examined under a fluorescence microscope.

Excitation and emission wavelengths were, respectively, 551 and 576 nm for MitoTracker Red and 490 and 525 nm for DCFDA and calcein-AM.

***Beclin 1* siRNA transfection.** Briefly, HeLa cells (5×10^5 per well) were seeded in six-well plates and incubated overnight. Random siRNA or *beclin 1* siRNA (Santa Cruz Biotechnology; 1.25 μg/well) was transfected using Lipofectamine 2000 (Invitrogen) according to the manufacturer's protocol. After 48 h, cells were collected, followed by immunoblot analysis, 4′-6-diamidino-2-phenylindole (DAPI) staining, or cell viability determination.

DAPI staining. *Beclin 1* siRNA–transfected HeLa cells were treated with DMSO or TAIII for 24 h. Both attached and floating cells were pooled, rinsed with PBS, fixed in 70% ethanol for 20 min, and then stained with DAPI (1.0 μg/mL) for 15 min. The cells were washed twice with PBS and then mounted onto slides. Cell morphology was examined under a fluorescence microscope. Moderately fluorescent and round nuclei were considered normal. Bright and condensed/fragmented nuclei were regarded as apoptotic.

Statistical analysis. Data were expressed as the mean ± SE of three determinations. Statistical analyses were done by using two-tailed Student's *t* test. $P \leq 0.05$ was considered statistically significant.

Results

TAIII is cytotoxic to cancer cells. TAIII exhibited cytotoxicity toward a panel of carcinoma cell lines including hepatocellular carcinoma cells (HepG2), human breast carcinoma cells (MCF-7), human nasopharyngeal carcinoma cells (SUNE-1), and human cervical epithelioid carcinoma cells (HeLa). The IC_{50} values ranged from 8.5 to 10.1 μmol/L after 48-hour incubation as determined by MTT assay. Sarsasapogenin was somewhat less cytotoxic with an IC_{50} of 56.4 μmol/L for HeLa cancer cells (Fig. 1*B*).

Autophagic vacuoles are observed in TAIII-treated cells. Inspection of TAIII-treated cells under a light microscope revealed the presence of microscopic vacuoles, which formed as early as 12 hours posttreatment (Fig. 2*A*). The number and size of the vacuoles increased progressively with the treatment time. The formation of vacuoles mediated by TAIII was not confined to HeLa cells but was also observed in HepG2 and SUNE-1 cancer cells. However, vacuoles were hardly observed in HeLa cells treated with sarsasapogenin. The ultrastructural details in TAIII-treated cells at 48 hours posttreatment were further examined by transmission electron microscopy (Fig. 2*B*). The formation of vacuoles was apparent when compared with DMSO control or sarsasapogenin-treated cells. The majority of vacuoles resemble autophagic vacuoles (autophagosomes and autolysosomes) and some of these presumably are membrane bound and contained cytoplasmic contents (21). These features are distinct from apoptotic cells, which are expected to exhibit cell shrinkage, nuclear fragmentation, and chromatin condensation (15). Careful examination of the transmission electron microscopy images revealed that some cells simultaneously possessed morphologies typical of both autophagy (autophagic vacuoles) and apoptosis (apoptotic nuclear condensation).

TAIII induces cellular translocation of LC3. LC3, a mammalian homologue of yeast *atg8*, is essential for autophagosome formation (22). The intracellular localization of LC3 in autophagic vacuoles induced by TAIII can be studied by transient transfection of cells with an expression plasmid of GFP-LC3 (23, 24). Fluorescence microscopic examinations were done at different time points to trace the redistribution of LC3 during autophagosome and autolysosome formations. In the DMSO control and sarsasapogenin-treated cells (Fig. 2*C*), GFP-LC3 was found predominantly as diffuse green fluorescence in the cytoplasm. However, in TAIII-treated cells, characteristic punctate fluorescent patterns were observed, indicating the recruitment of GFP-LC3 during autophagosome formation (9, 14, 22). The punctate feature representing the autophagosome gradually faded and finally vanished, presumably due to the fusion of autophagosome with lysosome (23), resulting in less GFP-LC3 located on the membrane. The incidence of autophagy induced by TAIII was quantified (Fig. 2*C*). The number of cells with punctate green fluorescence increased significantly with the treatment time of TAIII, indicating that TAIII mediated autophagy in a time-dependent manner.

TAIII induces LC3-II accumulation. LC3 exists in two forms. LC3-I residing in the cytosol is posttranslationally modified to the membrane-bound LC3-II, which is a structural component essential for autophagosome formation during autophagy (22). Immunoblot analyses of proteins from TAIII-treated cells revealed the presence of two bands, LC3-I and LC3-II (Fig. 2*D*). Weak bands corresponding to LC3-I were found in the DMSO controls whereas LC3-II was undetectable. The modification of LC3-I to LC3-II correlating to the extent of autophagosome formation (22) was observed as early as 12 hours posttreatment with 10 μmol/L TAIII. The degree of LC3-I to LC3-II conversion was initially low but significantly enhanced thereafter. The total LC3 expression levels were higher when TAIII treatment was prolonged or the dosages of TAIII were increased.

The increase in LC3-II expression can be associated with either an enhanced formation of autophagosome or an impaired autophagic degradation (25). To differentiate these two possibilities, LC3-II expression was assessed in the presence of bafilomycin A1, an inhibitor of V-ATPase that interferes with the fusion of autophagosome and lysosome and hence blocks the autophagic degradation including that of LC3-II (25). As shown in Fig. 2*D*, cells treated with TAIII or rapamycin, a prototypical autophagy inducer, had their LC3-II further accumulated in the presence of bafilomycin A1. These observations supported that the increased LC3-II expression mediated by TAIII was a consequence of exacerbated autophagosome formation. More importantly, these findings also indicated that TAIII might induce a complete autophagic flux.

TAIII induces oxidative stress. Oxidative stress is mediated by excessive ROS such as superoxide anion radical ($O_2^{\cdot-}$) and hydrogen peroxide (H_2O_2). The accumulation of these oxygen-derived species has been reported to promote cell death during autophagy and/or apoptosis (26–29). To examine whether oxidative stress was involved in TAIII-stimulated autophagy, we measured the intracellular ROS levels over a 48-hour period using cell permeable probe DHRh-123. As shown in Fig. 3*A*, untreated cells showed relatively constant basal levels of ROS whereas the TAIII-treated cells showed time- and dose-dependent elevations in ROS production. When cells were pretreated with the antioxidant *N*-acetylcysteine (NAC), ROS production was substantially inhibited.

SOD and catalase activities are up-regulated during TAIII treatment. The balance between ROS production and the capability of antioxidant defense system determines the extent of oxidative stress. SOD and catalase are essential enzymatic antioxidants capable of removing $O_2^{\cdot-}$ and H_2O_2, respectively. In this work, significant increases in SOD activities were evident during the course of TAIII treatment (Fig. 3*B*). Catalase activities were also correspondingly increased (Fig. 3*B*). However, overproduction of ROS was still observed (Fig. 3*A*) and the cellular antioxidant capacity seemed to be overwhelmed and oxidative stress might result.

NAC inhibits TAIII-mediated autophagy. The excessive ROS production has been suggested to play a role in the initiation of

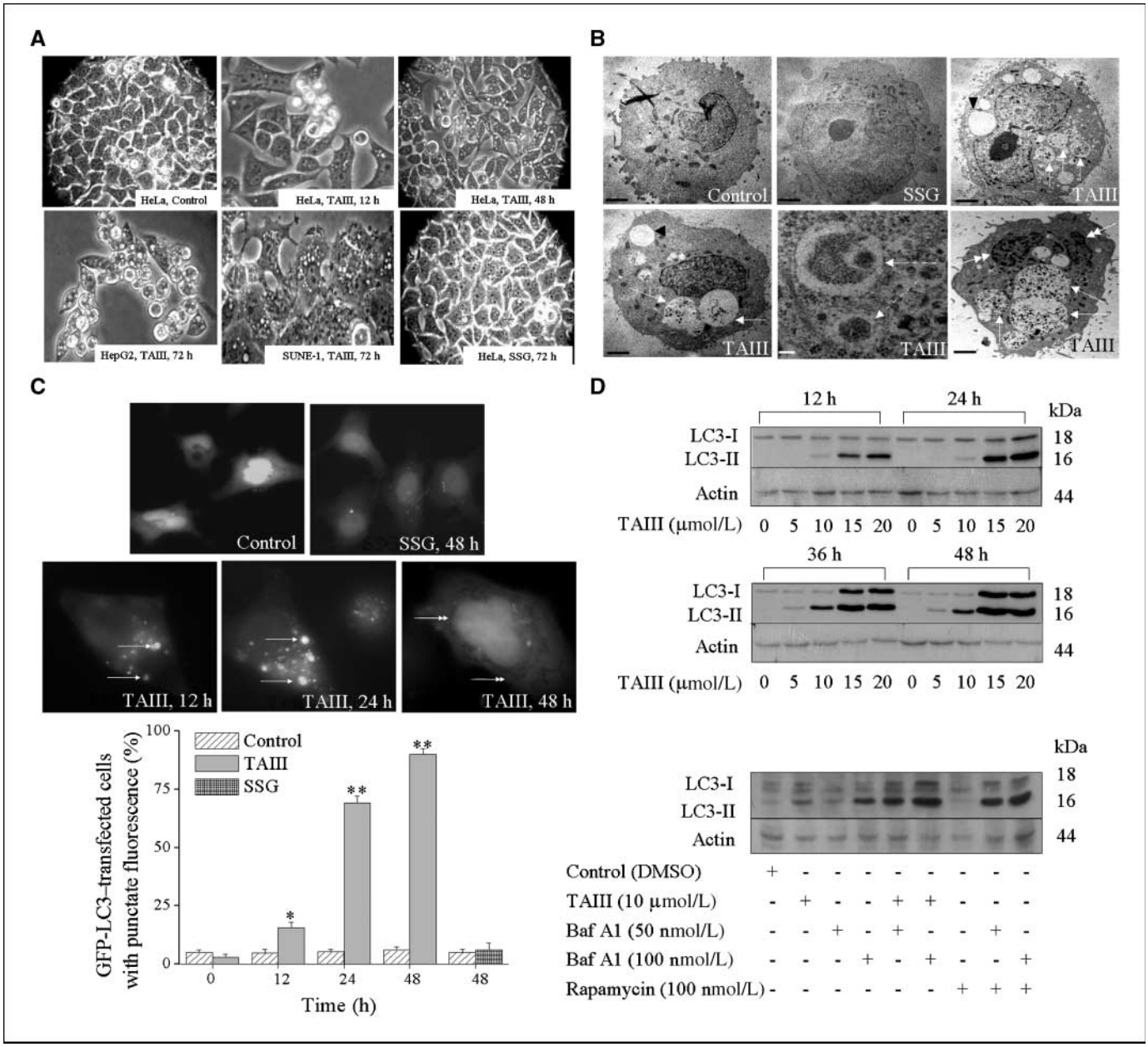

Figure 2. TAIII induces autophagy in HeLa cancer cells but sarsasapogenin does not. *A,* representative light microscopic images of different cancer cells treated with 10 μmol/L TAIII or 50 μmol/L sarsasapogenin. Magnification, ×20 or ×40. *B,* representative transmission electron microscopy images depicting ultrastructures of cells treated with DMSO, 50 μmol/L sarsasapogenin for 72 h, or 10 μmol/L TAIII for 48 h. *Arrows,* autophagic vacuoles. *Arrowheads,* empty vacuoles. *Dashed arrows,* membrane-bound autophagic vacuoles in TAIII treatment. *Double arrows,* invaginated and condensed nuclei. *Black bar,* 2 μm; *white bar,* 0.2 μm. *C,* cellular trafficking of GFP-LC3 during autophagosome and autolysosome formations in sarsasapogenin (50 μmol/L)– or TAIII (10 μmol/L)–treated cells at different time points as examined by fluorescence microscopy. *Single arrows,* autophagosomes. *Double arrows,* autolysosome in TAIII treatment at 48 h. Magnification, ×40. Autophagosome formation was quantified and data were presented as percentage of GFP-LC3–transfected cells with punctate fluorescence. A minimum of 100 GFP-LC3–transfected cells were counted. *, $P < 0.05$; **, $P < 0.001$, compared with DMSO control at the corresponding time points. *D,* Western blot analysis of the LC3 expression in cells treated with TAIII at various concentrations for 12 to 48 h (*top*). LC3 expression was also examined for cells treated with TAIII (10 μmol/L), rapamycin (100 nmol/L), or bafilomycin A1 (*Baf A1*; 50 or 100 nmol/L) for 48 h as indicated (*bottom*).

autophagy (17, 26). Hence, the antioxidative effect of NAC on TAIII-mediated autophagy was examined. The formation of microscopic vacuoles in TAIII-treated cells was significantly attenuated in the presence of NAC (Supplementary Fig. S1). NAC treatment also inhibited TAIII-mediated LC3-II expression as shown in Fig. 3*C*, providing evidence that ROS might stimulate the onset of autophagy.

Mitochondria are the sources of ROS generation. The source of ROS production in TAIII treatment is unclear but likely originated from mitochondrial respiratory activities. Therefore, the intracellular localization of ROS was examined by doubly staining cells with mitochondria-specific fluorescent marker MitoTracker Red and DCFDA. DCFDA is cell permeable and reacts preferentially with H_2O_2 to give fluorescent 2′,7′-dichlorofluorescin (DCF; ref. 26). As shown in Fig. 3*D*, TAIII-treated cells exhibited green punctate fluorescence of DCF whereas untreated cells showed substantially weaker signals. The merged DCF and MitoTracker Red image in

TAIII-treated cells showed a perfect overlap of fluorescence signals indicated by the orange coloration. These observations suggested that mitochondria were the sites of ROS overproduction.

TAIII decreases the mitochondrial membrane potential ($\Delta\psi_m$). Autophagic activity is involved in the removal of damaged organelles such as mitochondria (17, 21). To test whether mitochondrial perturbation was associated with TAIII-mediated autophagy, the mitochondrial membrane potential was measured using Rh-123, which is a lipophilic cation taken up by mitochondrial inner membrane and fluoresces in proportion to $\Delta\psi_m$. As shown in Fig. 4*A*, the control showed fairly constant $\Delta\psi_m$ values whereas TAIII induced a time- and dose-dependent decrease in $\Delta\psi_m$, evident as early as 2 hours posttreatment. Pretreatment with NAC did not affect the loss of $\Delta\psi_m$ (data not shown). These findings suggested that TAIII-mediated loss of $\Delta\psi_m$ was an early event and independent of ROS production.

TAIII induces MPT. The loss of $\Delta\psi_m$ may indicate an increase in MPT (30–32), which causes an increase in the membrane permeability to solutes with molecular mass <1.5 kDa. To test whether induction of MPT was associated with TAIII-mediated reduction in $\Delta\psi_m$, cells were treated with TAIII for 6 hours and the MPT was detected by an established method involving fluorescence staining with MitoTracker Red, calcein-AM, and $CoCl_2$ (33). In this method, calcein-AM is used as a membrane-permeable probe that can freely enter mitochondria. The exit of green fluorescent calcein from mitochondria, after being cleaved by intracellular esterases, is allowed only through the induction of MPT. Co^{2+} ions cannot readily enter mitochondria, but can be present in the cytoplasm and nucleus and quenches the calcein fluorescence therein as a result of Co^{2+}-calcein complex formation. In the presence of Co^{2+}, predominately the fluorescence of calcein trapped in mitochondria is imageable. Thus, as depicted in Fig. 4*B*, mitochondria in untreated cells accumulated calcein and were recognized as filamentous green fluorescence. The calcein signals in untreated cells could also be colocalized with the MitoTracker Red–labeled mitochondria, yielding a greenish-yellow coloration when the two images were merged. However, TAIII treatment resulted in loss of mitochondrial calcein fluorescence. In addition, the calcein and MitoTracker Red signals in TAIII-treated cells did not overlap well and the merged image was predominately MitoTracker Red signals. These observations could be interpreted as leakage of calcein from the mitochondria (33) resulting from induction of MPT by TAIII treatment. When cells were cotreated with TAIII and cyclosporin A, an inhibitor of MPT (28), the mitochondrial calcein was largely retained. Collectively, these observations illustrated that TAIII induced cyclosporin A–sensitive MPT.

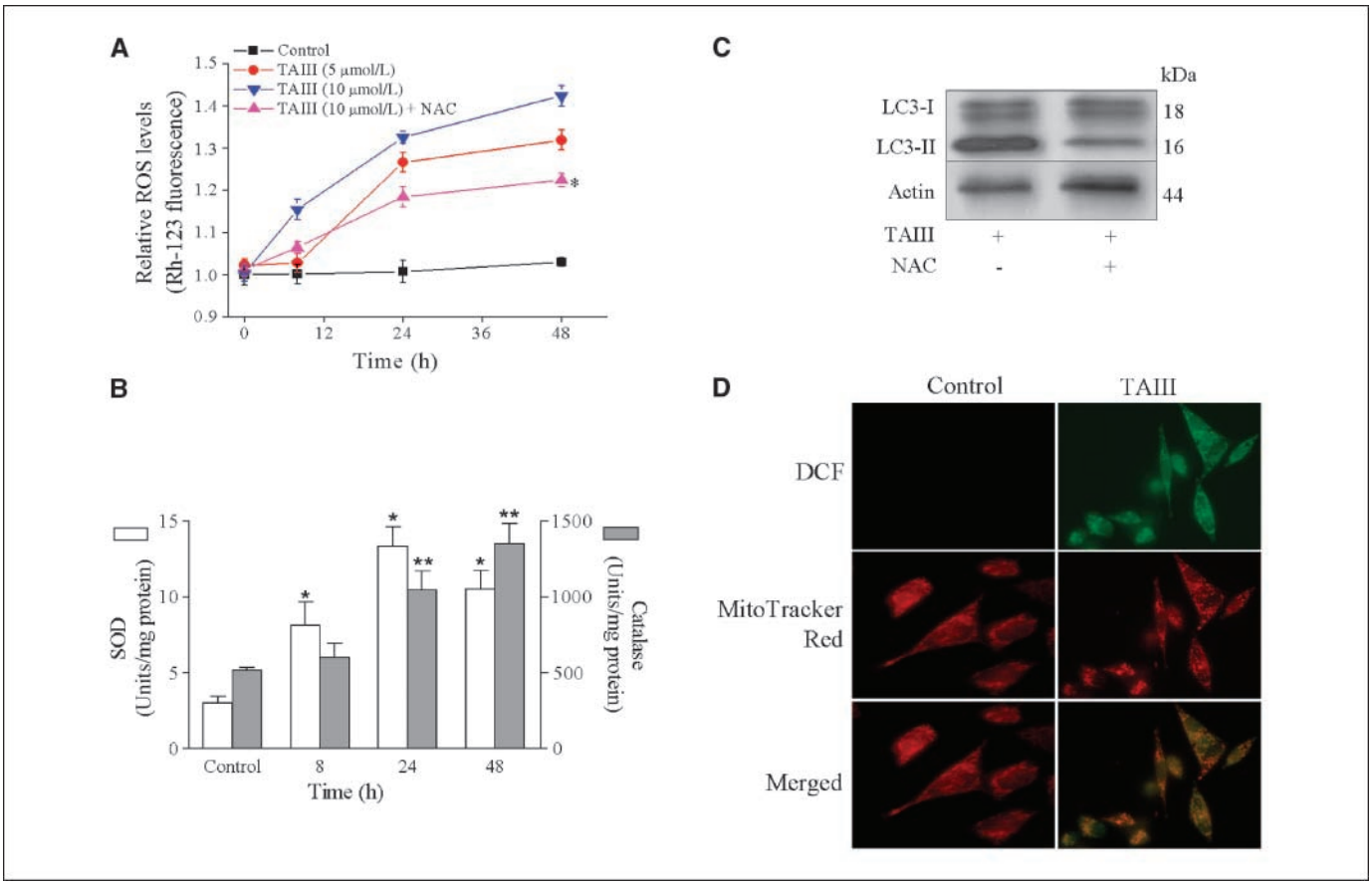

Figure 3. TAIII induces oxidative stress, which contributes to autophagy in HeLa cells. *A,* ROS levels were determined by fluorescence changes due to intracellular oxidation of nonfluorescent DHRh-123 to green fluorescent Rh-123. The addition of NAC (4 mmol/L, pretreated for 1 h) inhibited ROS generation. Data are expressed as fold increases relative to control at time 0. *, $P < 0.05$, compared with TAIII treatment (10 μmol/L) at the corresponding time points. *B,* SOD and catalase activities were determined for cells treated with 10 μmol/L TAIII. * and **, $P < 0.05$, compared with corresponding control. *C,* Western blot analysis of LC3-I and LC3-II expressions in cells treated with 10 μmol/L TAIII for 24 h in the absence or presence of NAC (4 mmol/L, pretreated for 1 h). *D,* cells treated with 10 μmol/L TAIII for 6 h were doubly stained with MitoTracker Red and DCFDA. The cell images were observed under a fluorescence microscope. Magnification, ×40.

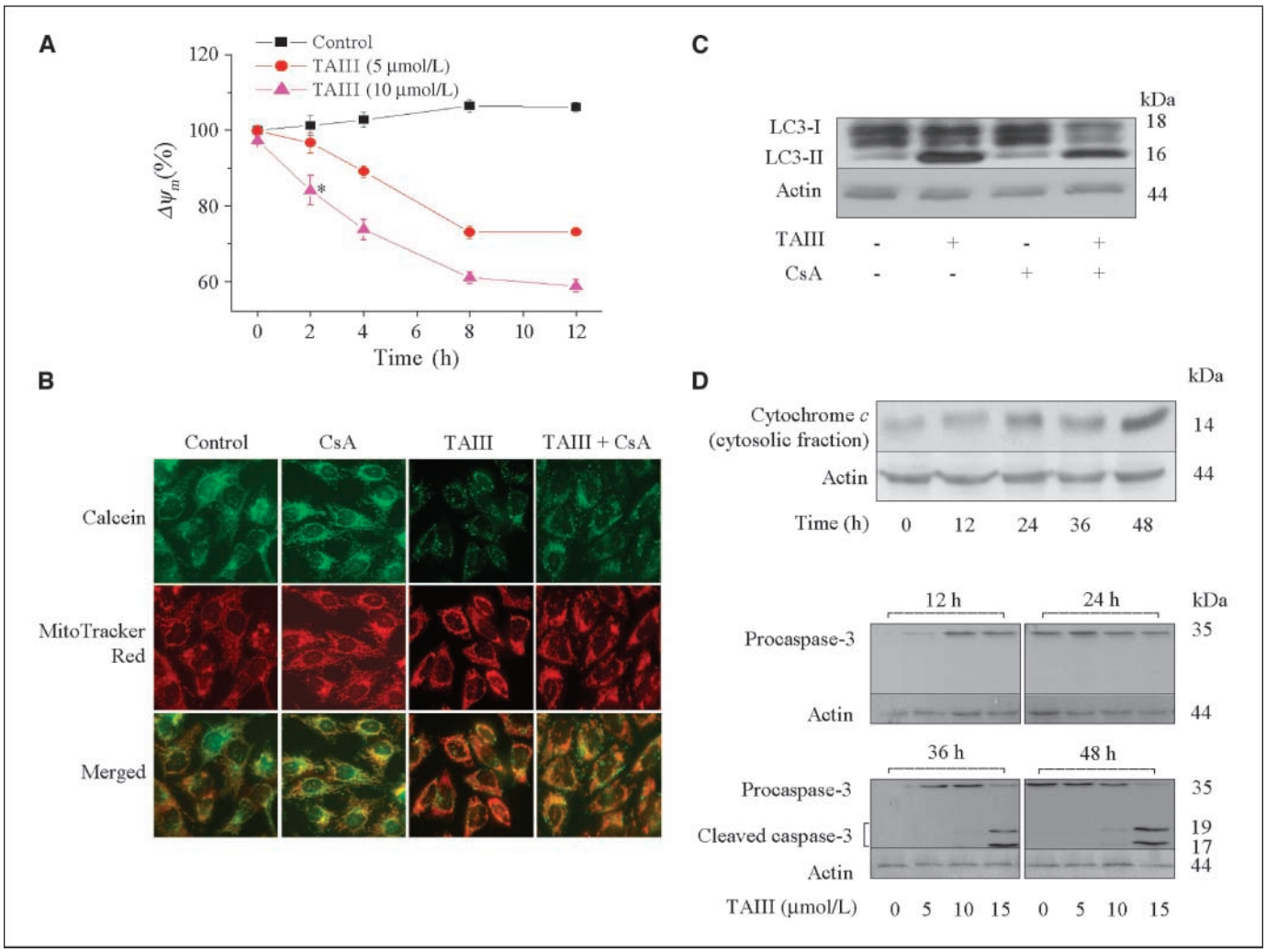

Figure 4. TAIII perturbs HeLa cell mitochondrial activities, which contributes to autophagy. *A,* changes of $\Delta\psi_m$ in cells treated with 5 μmol/L or 10 μmol/L of TAIII were measured as the fluorescence intensity of Rh-123 loaded to the cells. Control value at time 0 is set at 100%. *, $P < 0.05$, compared with the control at the corresponding time point. *B,* cells treated with 10 μmol/L TAIII for 6 h in the absence or presence of cyclosporin A (*CsA*; 2 μmol/L, pretreated for 1 h) were loaded with MitoTracker Red, calcein-AM, and $CoCl_2$ and then imaged by fluorescence microscope. Magnification, ×40. *C,* Western blot analysis showing that the conversion of LC3-I into LC3-II mediated by TAIII (10 μmol/L, 24 h) was reduced upon cyclosporine A treatment (2 μmol/L, pretreated for 1 h). *D,* Western blot analyses showing cytochrome *c* release into cytosol in cells treated with 10 μmol/L TAIII and caspase-3 expression in cells treated with 5 to 15 μmol/L of TAIII.

Cyclosporin A inhibits TAIII-mediated autophagy. The collapse of $\Delta\psi_m$ (Fig. 4*A*) in association with induction of MPT (Fig. 4*B*) in TAIII treatment seemed to be an early event leading to induction of autophagy. Therefore, the MPT inhibitory effect of cyclosporin A on autophagy was investigated. The formation of microscopic vacuoles in TAIII-treated cells was markedly reduced in the presence of cyclosporin A (Supplementary Fig. S2). Immunoblot analysis revealed that the conversion of LC3-I into LC3-II in TAIII-treated cells was also inhibited by cyclosporin A (Fig. 4*C*). These results indicated that the TAIII-elicited autophagy might be associated with an induction of MPT.

Cytochrome *c* is released and caspase-3 is cleaved after prolonged treatment with TAIII. Induction of MPT may lead to mitochondrial swelling, outer membrane rupture, and eventual release of intermembrane proapoptotic inducing factors such as cytochrome *c* (30). This is followed by the activation of caspase-9, which in turn mediates the cleavage of other executioner caspases (31). As shown in Fig. 4*D*, cells treated with TAIII (10 μmol/L) exhibited a time-dependent release of cytochrome *c* into cytosol. The release was most evident after prolonged drug treatment (48 hours). In addition, the proteolytic cleavage of caspase-3 in TAIII-treated cells was undetectable initially but could be detected after a 48-hour incubation (Fig. 4*D*), in coincidence with the release of cytochrome *c*. These results showed that TAIII treatment eventually caused apoptosis via an intrinsic mitochondrial pathway. It is noteworthy that caspase-3 cleavage could be considered as a late event (~ 48 hours) during the TAIII treatment, following the early induction (12 hours) of autophagic responses such as autophagic vacuole formation (Fig. 2*B*), GFP-LC3 recruitment (Fig. 2*C*), and LC3-II increase (Fig. 2*D*).

Inhibition of autophagy by 3-MA potentiates TAIII-mediated apoptotic cell death. The interconnection between TAIII-induced autophagy and apoptosis was further investigated using autophagy inhibitor 3-MA. 3-MA is a phosphoinositide 3-kinase inhibitor that exerts its autophagy-inhibiting effect before the formation of autophagosome during the early stages of autophagy (34). As depicted in Fig. 5*A* (and Supplementary Fig. S3), treatment of cells with 3-MA was effective in inhibiting the GFP-LC3 recruitment to

autophagosome. 3-MA at 10 mmol/L was only slightly toxic (Fig. 5*B*) but exhibited a significant inhibitory effect on autophagosome formation, as also noted in previous studies (35–38). However, the IC_{50} of TAIII after a 24-hour treatment decreased 5-fold from 15.9 to 2.9 μmol/L in the presence of 3-MA (Fig. 5*B*). At this early time point, HeLa cells pretreated with 3-MA followed by TAIII not only showed cell shrinkage (Supplementary Fig. S3) but also exhibited significant cleavages of the proapoptotic caspase-9 and caspase-3, whereas cells exposed to either compound alone did not (Fig. 5*C*). Collectively, these results suggested that 3-MA inhibited TAIII-mediated autophagy and it also sensitized the cells to the cytotoxic actions of TAIII with induction of apoptosis.

Inhibition of autophagy by *beclin 1* siRNA increases the cytotoxic sensitivity of cells to TAIII. The gene product of *beclin 1*, also known as the mammalian orthologue of yeast autophagic gene *atg6*, is a component of class III phosphatidylinositol 3-kinase complex essential for autophagosome formation (35). In this study, the role of autophagy in the TAIII-mediated cytotoxicity was studied by knocking down the *beclin 1* expression using siRNA. The expression of Beclin 1 was markedly suppressed in HeLa cells transfected with *beclin 1* siRNA but not those with random siRNA (Fig. 6*A*). Accordingly, cells transfected with *beclin 1* siRNA showed much reduced level of autophagosome formation after TAIII treatment when compared with those transfected with random siRNA (Fig. 6*B*; Supplementary Fig. S4), indicating that *beclin 1* promoted TAIII-induced autophagy. Notably, the IC_{50} of TAIII was significantly decreased from 16.4 to 11.2 μmol/L by *beclin 1* siRNA but not affected by random siRNA (IC_{50}, 15.7 μmol/L; Fig. 6*C*). The degree of apoptosis was also determined by DAPI staining (Supplementary Fig. S5). Apoptotic cell demise with condensed or fragmented nuclei was most remarkable in *beclin 1* siRNA–transfected cells treated with TAIII. Quantification of apoptotic cell corpses showed that the incidence of apoptosis after TAIII treatment was 3-fold more in *beclin 1* siRNA–transfected cells when compared with random siRNA control (Fig. 6*D*). Taken together, these findings suggested that the cytotoxic effect of TAIII was potentiated by down-regulation of *beclin 1* with enhancement of apoptosis. These observations supported the notion that autophagy mediated by TAIII was protective in nature.

Discussion

A. asphodeloides is listed in Chinese Pharmacopoeia and has been widely used in China and Japan for medicinal purposes due to its rich content of saponins (3, 4). In the present study, we report that the naturally occurring saponin TAIII from *A. asphodeloides* is a strong inducer to autophagy (Fig. 2) as well as to apoptosis (Fig. 4). These two processes, autophagy and apoptosis, although mechanistically different, are sequentially triggered by TAIII via the mitochondria-dependent pathway (Figs. 3 and 4). From the literature, the switch between autophagy and apoptosis is complicated and poorly defined. Autophagy and apoptosis can be induced in response to cellular stresses in a number of ways such that the induction of autophagy/apoptosis can occur sequentially, simultaneously, or in a mutually exclusive manner (11, 14, 39, 40). It has been shown through a gene expression profiling approach that autophagy and apoptosis occurred concomitantly, wherein multiple apoptotic genes were up-regulated together with autophagic genes (39). Defensive autophagy was induced in sulforaphane-treated human prostate cancer cells to antagonize apoptosis (14). Apoptosis was not induced in arsenic trioxide–treated human glioma cells until autophagic cell death was inhibited by bafilomycin A1 (11). In contrast, autophagy was triggered only when apoptosis was blocked by the pan-caspase inhibitor in both neurons and HeLa cells (40).

Inhibition of autophagy by treatment with 3-MA (Fig. 5) or siRNA against autophagic gene *beclin 1* (Fig. 6) enhanced the apoptotic cell death, suggesting that TAIII-mediated autophagy has a cytoprotective role in nature. The role of autophagy in cancer cells has emerged as an important topic of intense debate, with opinions split on whether it acts as a self-defensive or a self-destructive mechanism. Cancer cells undergoing nutrient starvation (7), hypoxia (8), ionizing radiation (9, 10), temozolomide (12),

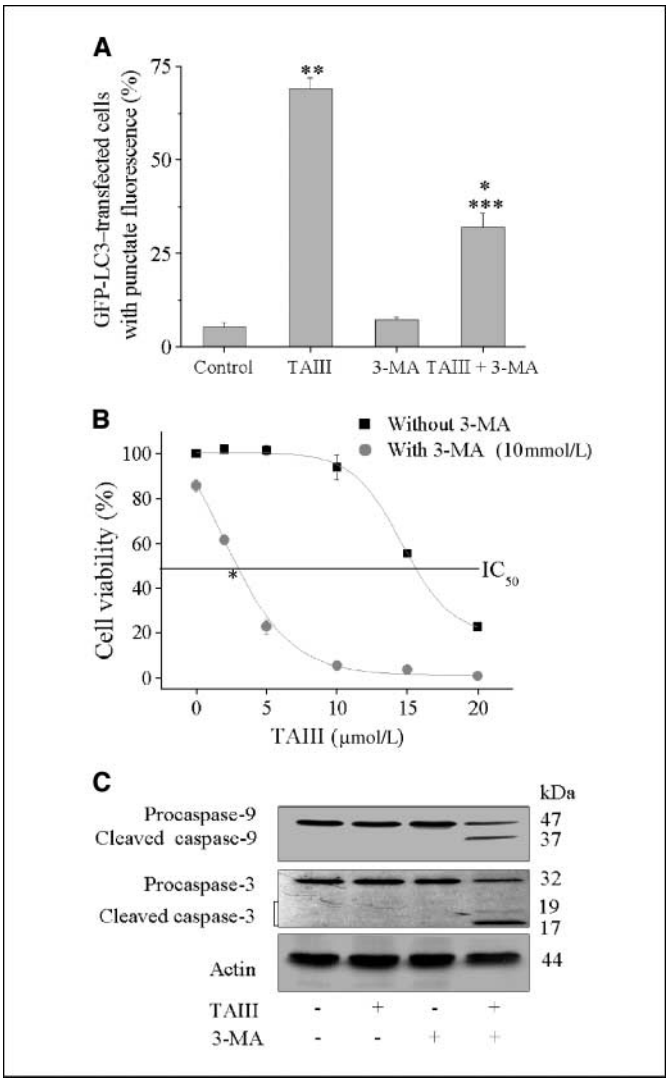

Figure 5. 3-MA inhibits autophagy and sensitizes HeLa cells to cytotoxic actions of TAIII. *A,* autophagosome formation in GFP-LC3–transfected cells treated with 10 μmol/L TAIII for 24 h in the absence or presence of 3-MA (10 mmol/L, pretreated for 2 h) was quantified. Data were presented as percentage of GFP-LC3–transfected cells with punctate fluorescence. A minimum of 100 GFP-LC3-transfected cells were counted. *, $P < 0.05$; **, $P < 0.001$, compared with control. ***, $P < 0.05$, compared with TAIII treatment. *B*, cell viability was determined by MTT assay after treatment with various concentrations of TAIII for 24 h in the absence or presence of 3-MA (10 mmol/L, pretreated for 2 h). *, $P < 0.001$, compared with the IC_{50} of TAIII treatment without 3-MA. *C,* Western blot analyses of caspase-9 and caspase-3 expressions in cells treated with 10 μmol/L TAIII for 24 h in the absence or presence of 3-MA (10 mmol/L, pretreated for 2 h).

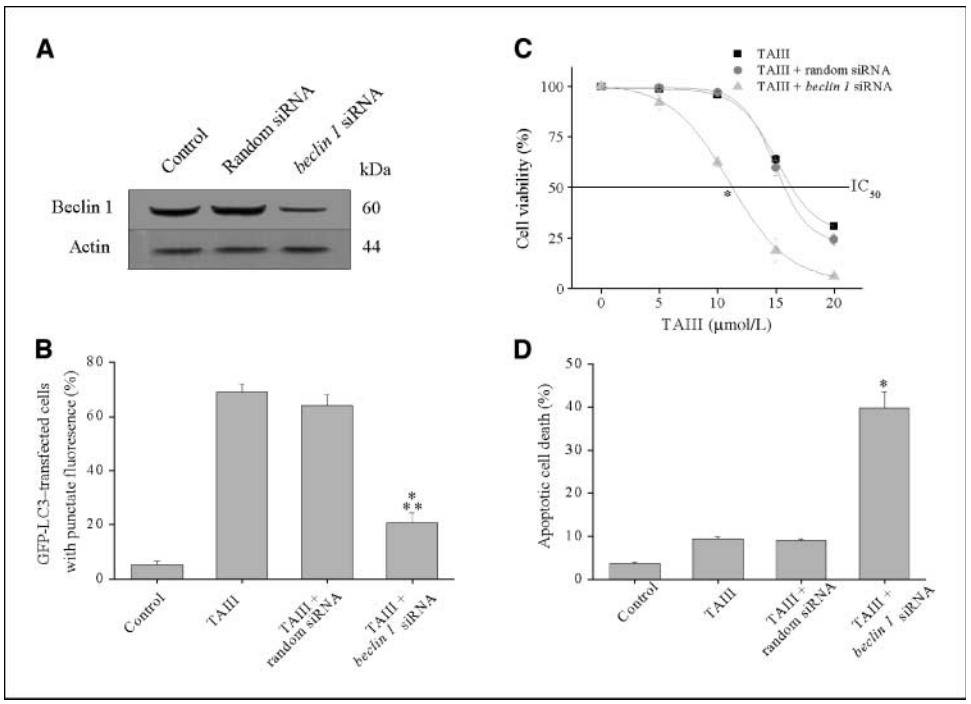

Figure 6. *Beclin 1* siRNA inhibits autophagosome formation and enhances the cytotoxicity induced by TAIII in HeLa cells. *A,* Western blot of Beclin 1 protein expression in untransfected cells or cells transfected with random siRNA or *beclin 1* siRNA for 48 h. *B,* autophagosome formation in cells cotransfected with *beclin 1* siRNA and GFP-LC3 and treated with 10 μmol/L TAIII for 24 h was quantified. Data were presented as percentage of GFP-LC3–transfected cells with punctate fluorescence. A minimum of 100 GFP-LC3–transfected cells were counted. *, $P < 0.05$, compared with random siRNA; **, $P < 0.001$, compared with TAIII treatment. *C,* cell viability was determined by MTT assay. siRNA-transfected cells were treated with 10 μmol/L TAIII for 24 h. *, $P < 0.05$, compared with the IC_{50} of TAIII treatment. *D,* apoptotic cell demise was determined by DAPI nuclear staining. siRNA-transfected cells were treated with DMSO or 10 μmol/L TAIII for 24 h. A minimum of 100 DAPI-stained cells were counted. *, $P < 0.05$, compared with TAIII treatment or random siRNA.

and sulforaphane (14) treatments manifested the defensive role of autophagy in contrast to the destructive role displayed by arsenic trioxide– (11), resveratrol- (13), tamoxifen- (19), and ceramide-induced (41) autophagy. All these arguments about the role of autophagy in cancer cells have received supports (6, 21). Shintani and Klionsky (15) suggested that the consequences of autophagy are dependent on the physiologic contexts.

In this study, TAIII treatment markedly induced ROS production, which has been suggested to be essential for both autophagy and apoptosis (26, 27). The origin of the TAIII-mediated overproduction of ROS (Fig. 3*A*) is unclear but may be related to the drug-induced dysfunction of mitochondria, which were the major sites of intracellular ROS production (Fig. 3*D*). On the other hand, a rapid loss of $\Delta\psi_m$ (Fig. 4*A*) was also detected early during the TAIII treatment, paralleled by the activation of MPT (Fig. 4*B*). The mechanism by which TAIII-induced mitochondrial membrane destabilization may be due to the membrane-perturbing property of this spirostanol saponin (42, 43). The hydrophobic aglycone (sarsasapogenin) in TAIII probably aids in traversing the membrane and affects the mitochondrial functions (44). The accumulation of ROS and activation of MPT during TAIII treatment may jointly initiate autophagic response as suggested by the observations that antioxidant (NAC) or MPT inhibitor (cyclosporin A) suppressed the autophagy induction (Figs. 3*C* and 4*C*). Although the signal transduction pathway leading to activation of autophagy is not fully resolved, it has been reported that ROS, particularly H_2O_2, are signaling molecules essential for starvation-induced autophagy. The cysteine protease HsAtg4 has been shown to be a direct target for oxidation by H_2O_2 (26).

According to Lemasters's model (28, 29), the promotion of MPT is a crucial factor controlling the cellular fate by adopting autophagy or apoptosis. Therefore, we hypothesize that during the early stages of TAIII treatment, the degree of MPT induced is relatively low, and thus self-defensive autophagy occurs for turnover of damaged mitochondria. However, after TAIII treatment is prolonged or the dosage is increased, the augmented MPT attains a "threshold," at which time autophagy is extensive and followed by apoptosis. The defensive effect exerted by autophagy is then diminished and the extent of apoptosis increases (compare Figs. 2*B* and 4*D*). In this respect, autophagy seems to retard the occurrence of apoptosis. This notion is further supported by our findings that the inhibition of autophagy by 3-MA or more specifically by *beclin 1* siRNA increased cell sensitivity to TAIII-mediated apoptosis (Figs. 5 and 6). *Beclin 1*, probably the first identified mammalian gene with a role in mediating autophagy (35), is monoallelically deleted in 40% to 75% of sporadic human breast cancers and ovarian cancers (45). On the other hand, Beclin 1 protein has been reported to form complex with antiapoptotic protein CED-9/Bcl-2, and on its down-regulation by siRNA, apoptosis is triggered (37). Hence, Beclin 1 seems to be a tumor suppressor having a role in connecting autophagic and apoptotic machineries. The release of cytochrome *c* into the cytosol in TAIII-treated cells (Fig. 4*D*) owing to the disruption of mitochondrial membrane signals the onset of apoptosis. The released cytochrome *c* binds to the adaptor molecule Apaf-1 to form the apoptosome complex that activates caspase-9, leading to cleavage of caspase-3 (Fig. 4*D*), the "executioner" protease of apoptosis (30, 46). The release of cytochrome *c* is therefore a critical point, after which autophagy progresses irreversibly to apoptosis.

The connectivity between autophagy and apoptosis in TAIII treatment is regulated by mitochondrial activities (Figs. 3 and 4). Overproduction of ROS, disruption of mitochondrial membrane, induction of cyclosporin A–sensitive MPT, and cytochrome *c* release are all consistent with the inner mitochondrial membrane being the possible molecular target of TAIII (44). Molecular docking has been used to investigate the possible interactions between TAIII/sarsasapogenin and the inner membrane-associated components of the MPT pore, such as cyclophilin D. Preliminary data show that TAIII can be docked into cyclophilin

D whereas sarsasapogenin cannot. Sarsasapogenin lacks sugar moiety, and this may possibly explain its insignificant induction of autophagy and relatively weak cytotoxicity. Further experiments are warranted to examine the presumed interaction between TAIII/sarsasapogenin and cyclophilin D.

In conclusion, our study showed that the natural substance TAIII is an autophagy- and apoptosis-inducing agent to cancer cells. However, such dual properties possessed by TAIII have not been reported for other saponins such as dioscin and polyphyllin D. This represents a challenging task for medicinal chemists to work out the relationship between saponin structures and bioactivities. The interaction of saponin with mitochondrial membrane components will be of particular interest.

Disclosure of Potential Conflicts of Interest

No potential conflicts of interest were disclosed.

Acknowledgments

Received 6/13/2008; revised 9/26/2008; accepted 10/15/2008.

Grant support: Small Project Funding Programme (to Dr. Lai-King Sy) of the University of Hong Kong and the Area of Excellence Scheme (AoE/P-10/01) administered by the University Grants Committee at the University of Hong Kong.

The costs of publication of this article were defrayed in part by the payment of page charges. This article must therefore be hereby marked *advertisement* in accordance with 18 U.S.C. Section 1734 solely to indicate this fact.

We thank Dr. Rory M. Watt for his help in editing the manuscript and Department of Health, HKSAR, China, for providing information about the *Anemarrhena asphodeloides*.

References

1. Wang Y, Cheung YH, Yang Z, Chiu JF, Che CM, He QY. Proteomic approach to study the cytotoxicity of dioscin (saponin). Proteomics 2006;6:2422–32.
2. Lee MZ, Chan JYW, Kong SK, et al. Effects of polyphyllin D, a steroidal saponin in *Paris polyphylla*, in growth inhibition of human breast cancer cells and in xenograft. Cancer Biol Ther 2005;4:1248–54.
3. Zhang J, Meng Z, Zhang M, Ma D, Xu S, Kodama H. Effect of six steroidal saponins isolated from *Anemarrhenae* rhizoma on platelet aggregation and hemolysis in human blood. Clin Chim Acta 1999;289:79–88.
4. Zhang J, Zhang M, Sugahara K, et al. Effect of steroidal saponins of *Anemarrhenae* rhizoma on superoxide generation in human neutrophils. Biochem Biophys Res Commun 1999;259:636–9.
5. Wang GJ, Lin LC, Chen CF, et al. Effect of timosaponin A-III, from *Anemarrhenae asphodeloides* Bunge (Liliaceae), on calcium mobilization in vascular endothelial and smooth muscle cells and on vascular tension. Life Sci 2002;71:1081–90.
6. Mizushima N, Levine B, Cuervo AM, Klinosky DJ. Autophagy fights disease through cellular self-digestion. Nature 2008;451:1069–75.
7. Eskelinen, EL. Maturation of autophagic vacuoles in mammalian cells. Autophagy 2005;1:1–10.
8. Semenza GL. Mitochondrial autophagy: life and breath of the cell. Autophagy 2008;4:534–6.
9. Ito H, Daido S, Kanzawa T, Kondo S, Kondo Y. Radiation-induced autophagy is associated with LC3 and its inhibition sensitizes malignant glioma cells. Int J Oncol 2005;26:1401–10.
10. Paglin S, Hollister T, Delohery T, et al. A novel response of cancer cells to radiation involves autophagy and formation of acidic vesicles. Cancer Res 2001;61:439–44.
11. Kanzawa T, Kondo Y, Ito H, Kondo S, Germano I. Induction of autophagic cell death in malignant glioma cells by arsenic trioxide. Cancer Res 2003;63:2103–8.
12. Kanzawa T, Germano IM, Komata T, Ito H, Kondo Y, Kondo S. Role of autophagy in temozolomide-induced cytotoxicity for malignant glioma cells. Cell Death Differ 2004;11:448–57.
13. Opipari AW, Tan L, Boitano AE, Sorenson DR, Aurora A, Liu JR. Resveratrol-induced autophagocytosis in ovarian cancer cells. Cancer Res 2004;64:696–703.
14. Herman-Antosiewicz A, Johnson DE, Singh SV. Sulforaphane causes autophagy to inhibit release of cytochrome *c* and apoptosis in human prostate cancer cells. Cancer Res 2006;66:5828–35.
15. Shintani T, Klionsky DJ. Autophagy in health and disease: a double-edged sword. Science 2004;306:990–5.
16. Nishino I, Fu J, Tanji K, et al. Primary LAMP-2 deficiency causes X-linked vacuolar cardiomyopathy and myopathy (Danon disease). Nature 2000;406:906–10.
17. Jin S. Autophagy, mitochondrial quality control, and oncogenesis. Autophagy 2006;2:80–4.
18. Nixon RA. Autophagy in neurodegenerative disease: friend, foe or turncoat? Trends Neurosci 2006;29:528–35.
19. Bursch W, Ellinger A, Kienzl H, et al. Active cell death induced by the antiestrogens tamoxifen and ICI 164 384 in human mammary carcinoma cells (MCF-7) in culture: the role of autophagy. Carcinogenesis 1996;17:1595–607.
20. Guertin DA, Sabatini DM. An expanding role for mTOR in cancer. Trends Mol Med 2005;11:353–61.
21. Kelekar A. Autophagy. Ann N Y Acad Sci 2005;1066:259–71.
22. Kabeya Y, Mizushima N, Ueno T, et al. LC3, a mammalian homologue of yeast Apg8p, is localized in autophagosome membranes after processing. EMBO J 2000;19:5720–8.
23. Mizushima N, Yamamoto A, Matsui M, Yoshimori T, Ohsumi Y. *In vivo* analysis of autophagy in response to nutrient starvation using transgenic mice expressing a fluorescent autophagosome marker. Mol Biol Cell 2004;15:1101–11.
24. Köchl R, Hu XW, Chan EYW, Tooze SA. Microtubules facilitate autophagosome formation and fusion of autophagosomes with endosomes. Traffic 2006;7:129–45.
25. Klionsky DJ, Abeliovich H, Agostinis P, et al. Guidelines for the use and interpretation of assays for monitoring autophagy in higher eukaryotes. Autophagy 2008;4:1–25.
26. Scherz-Shouval R, Shvets E, Fass E, Shorer H, Gil L, Elazar Z. Reactive oxygen species are essential for autophagy and specifically regulate the activity of Atg4. EMBO J 2007;26:1749–60.
27. Singh SV, Srivastava SK, Choi S, et al. Sulforaphane-induced cell death in human prostate cancer cells is initiated by reactive oxygen species. J Biol Chem 2005;280:19911–24.
28. Lemasters JJ, Nieminen AL, Qian T, et al. The mitochondrial permeability transition in cell death: a common mechanism in necrosis, apoptosis and autophagy. Biochim Biophys Acta 1998;1366:177–96.
29. Rodriguez-Enriquez S, He L, Lemasters JJ. Role of mitochondrial permeability transition pores in mitochondrial autophagy. Int J Biochem Cell Biol 2004;36:2463–72.
30. Ly JD, Grubb DR, Lawen A. The mitochondrial membrane potential ($\Delta\psi_m$) in apoptosis; an update. Apoptosis 2003;8:115–28.
31. Kroemer G, Reed JC. Mitochondrial control of cell death. Nat Med 2000;6:513–9.
32. Costantini P, Jacotot E, Decaudin D, Kroemer G. Mitochondrion as a novel target of anticancer chemotherapy. J Natl Cancer Inst 2000;92:1042–53.
33. Li L, Han W, Gu Y, et al. Honokiol induces a necrotic cell death through the mitochondrial permeability transition pore. Cancer Res 2007;67:4894–903.
34. Seglen PO, Gordon PB. 3-Methyladenine: specific inhibitor of autophagic/lysosomal protein degradation in isolated rat hepatocytes. Proc Natl Acad Sci U S A 1982;79:1889–92.
35. Liang XH, Jackson S, Seaman M, et al. Induction of autophagy and inhibition of tumorigenesis by *beclin 1*. Nature 1999;402:672–6.
36. Abedin MJ, Wang D, McDonnell MA, Lehmann U, Kelekar A. Autophagy delays apoptotic death in breast cancer cells following DNA damage. Cell Death Differ 2007;14:500–10.
37. Boya P, González-Polo RA, Casares N, et al. Inhibition of macroautophagy triggers apoptosis. Mol Cell Biol 2005;25:1025–40.
38. Shimizu S, Kanaseki T, Mizushima N, et al. Role of Bcl-2 family proteins in a non-apoptotic programmed cell death dependent on autophagy genes. Nat Cell Biol 2004;6:1221–8.
39. Gorski SM, Chittaranjan S, Pleasance ED, et al. A SAGE approach to discovery of genes involved in autophagic cell death. Curr Biol 2003;13:358–63.
40. Xue L, Fletcher GC, Tolkovsky AM. Mitochondria are selectively eliminated from eukaryotic cells after blockade of caspases during apoptosis. Curr Biol 2001;11:361–5.
41. Daido S, Kanzawa T, Yamamoto A, Takeuchi H, Kondo Y, Kondo S. Pivotal role of the cell death factor BNIP3 in ceramide-induced autophagic cell death in malignant glioma cells. Cancer Res 2004;64:4286–93.
42. Wang Y, Che CM, Chiu JF, He QY. Dioscin (saponin)-induced generation of reactive oxygen species through mitochondria dysfunction: a proteomic-based study. J Proteome Res 2007;6:4703–10.
43. Francis G, Kerem Z, Makkar HPS, Becker K. The biological action of saponins in animal systems: a review. Br J Nutr 2002;88:587–605.
44. Haridas V, Higuchi M, Jayatilake GS, et al. Avicins: Triterpenoid saponins from *Acacia victoriae* (Bentham) induce apoptosis by mitochondrial perturbation. Proc Natl Acad Sci U S A 2001;98:5821–6.
45. Aita VM, Liang XH, Murty VV, et al. Cloning and genomic organization of beclin 1, a candidate tumor suppressor gene on chromosome 17q21. Genomics 1999;59:59–65.
46. Riedl SJ, Salvesen GS. The apoptosome: signalling platform of cell death. Nat Rev Mol Cell Biol 2007;8:405–13.

Timosaponin A-III Induces Autophagy Preceding Mitochondria-Mediated Apoptosis in HeLa Cancer Cells

Lai-King Sy, Siu-Cheong Yan, Chun-Nam Lok, et al.

Cancer Res 2008;68:10229-10237.